JOURNAL OF MATERIALS SCIENCE 32 (1997) 2087–2092

Viscosity and structure variations of Al–Si alloy in the semi-solid state

Y. S. YANG, C.-Y. A. TSAO
Department of Materials Science and Engineering (24), National Cheng Kung University, Tainan, Taiwan

The viscosity and microstructure evolution of A356 Al–Si alloy in the semi-solid state were investigated. During continuous cooling, the viscosity increases slowly at the onset of the semi-solid region, and starts to increase abruptly after reaching a critical temperature. The higher the shear rate, the lower is the critical temperature. During isothermal stirring, the viscosity decreases and the sphericity increases as the shear rate increases. The grain size decreases and the sphericity increases as the shear rate increases for short stirring times. The viscosity increases as the temperature decreases during isothermal stirring. The spheroidizing effect is not significant for short stirring time. During isothermal stirring, the viscosity increases as the rest time increases. Both the grain size and sphericity increase as the rest time, following stirring, increases. The coarsening exponent is 3.2, suggesting that the coarsening is controlled by the volume diffusion of the grains. During isothermal stirring, the viscosity decreases as the stirring time increases. The sphericity increases and the grain size decreases as the stirring time increases. We propose that there is a critical stirring time, above which the grain size increases with stirring time, but below which the grain size decreases with stirring time.

1. Introduction

Porosity and segregation are the most common defects that affect the mechanical properties of the castings. Recently, an advanced process, the semi-solid process (SSP), has emerged to reduce these defects and to obtain better structure and mechanical properties [1–5]. Compared with conventional cast materials, SSP materials have less segregation and porosity, and finer grain size. In practice, SSP can increase part-forming rate, reduce the thermal shock imposed on the mould, increase mould life, etc. [2].

In 1971, Spencer *et al.* [6] applied a shear strain on a solidifying Sn–15% Pb alloy, and discovered a remarkable reduction in shear stress compared with those that were not sheared during solidification, which pioneered study on the behaviour of metals in the semi-solid state. The sheared alloy showed a non-dendritic structure, as opposed to the dendritic structure of un-sheared alloy. Since this early work, SSP has become a widely studied and accepted process. SSP has the following characteristics: non-dendritic structure, shorter solidification time, less segregation, less shrinkage porosity, less energy consumption, and less tooling deterioration.

In this study, the physical properties, namely viscosity and thixotropic behaviour, and microstructure evolution of A356 Al–Si alloy in the semi-solid state, were investigated. The A356 Al–Si alloy has the following characteristics; good castability and mechanical properties, light weight and a better oxidation resistance, and is widely used [7–13]. A considerably wide semi-solid regime that is suitable for the studies on semi-solid behaviour is also provided by the A356 Al–Si alloy. The relationships between viscosity, shear rate, continuous cooling and stirring, isothermal stirring, stirring temperature, stirring time and rest time after stirring, were studied. In addition, the evolution of the non-dendritic structure of A356 alloy during the semi-solid processing was investigated.

2. Experimental procedure

A Shearl type of Rheometer was used to measure the viscosity and to produce the semi-solid slurry. The liquid flow within the viscometer needed to be laminar. The Reynolds number was calculated to be around 78 for the process parameters used, which was less than 1900, and according to Bird *et al.* the liquid flow within the viscometer was laminar [14].

The alloy studied was A356 Al–Si alloy, the nominal chemical composition of which was (wt%) 7.0% Si–0.35% Mg–0.2% Fe (max)–0.2% Cu (max)–0.1% Zn (max)–Al (bal.). The nominal solidus and liquidus were 830 and 886 K, respectively.

The effects of shear rate and temperature on the viscosity of A356 alloy during continuous cooling in the semi-solid state were studied. The effects of shear rate and temperature on the viscosity during isothermal stirring were also studied. The variations of viscosity with rest time after stirring at a given temperature, and the variations of viscosity with stirring time at a given temperature, were also investigated.

0022–2461

The samples were taken during the experiment to study the effects of isothermal stirring temperature, shear rate, stirring time and rest time on the structure evolution, grain size and sphericity, and the Oswald ripening phenomenon of A356 alloy in the semi-solid state. Metallographic samples were prepared using the standard metallographic preparation method. The etching solution was 2% HF. IA software from Optimas was used for image analyses. The two-dimensional sphericity analyses were calculated to be $4\pi a/b^2$, where a and b are the area and the perimeter of the grains measured from the micrographs, respectively. The average grain sphericity was calculated to be Σ sphericity/n, where n is the total number of the grains.

3. Results and discussion

Fig. 1 shows the variations of viscosity of A356 alloy with temperatures for various shear rates during continuous cooling. The A356 alloy was superheated 50 K over the liquidus, at which temperature the melt was held for 5 min before being continuously cooled at a rate of 0.5 K min^{-1}. The viscosity increases as the temperature decreases. However, the viscosity increases slowly at the onset of the semi-solid region, and starts to increase abruptly after reaching a critical temperature for all three shear rates. This critical temperature is believed to correspond to the coherent temperature, at which the dendritic network is formed. It is shown that the higher the shear rate, the lower is the critical temperature, due to breakdown of the dendrite network by the higher shear rate. It suggests that even with a high solid fraction, the viscosity of the melt can still be very low when a higher shear rate is applied.

The effect of shear rate on the viscosity of A356 alloy is plotted in Fig. 2. The A356 alloy was superheated 50 K over the liquidus, at which temperature the melt was held for 5 min before cooling to 873 K at a rate of 0.5 K min^{-1}. The melt was isothermally stirred for 60 s at 36, 95, 119, 142 and 178 s^{-1} shear rates, respectively, and then held unstirred for 15 s before the viscosity was measured and the samples were taken. The viscosity decreases as the shear rate increases due to fragmentation and spheroidization of dendritic crystals. Fig. 3 shows the corresponding micrographs for 95, 119 and 142 s^{-1} shear rates, respectively. A large rosette type of structure is shown for the lower shear rate of 95 s^{-1}. As the shear rate increases, the rosette type of structure breaks up into individual crystals, which gives a spheroidized non-dendritic structure with less liquid entrapped inside.

In the initial stage of stirring, a "rosette" type of structure would form due to bending and plastic deformation of the dendrites [2] as shown in Fig. 3a. At this stage, the dendrites formed are fragmented into smaller particles and the shearing and abrasion among grains lead to a more equiaxed structure. Spheroidization of the particles also takes place, driven by the reduction of the interfacial energy between particles and liquid. In addition, solutes diffuse from small particles to larger particles due to the Gibbs–Thomson

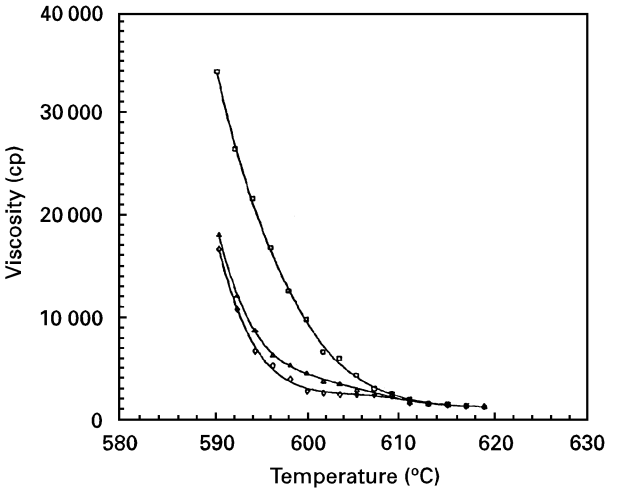

Figure 1 Variations of viscosity with temperature for different shear rates during continuous cooling at 0.5 °C min^{-1}. Shear rates: (□) 36 s^{-1}, (▲) 95 s^{-1}, (◇) 119 s^{-1}.

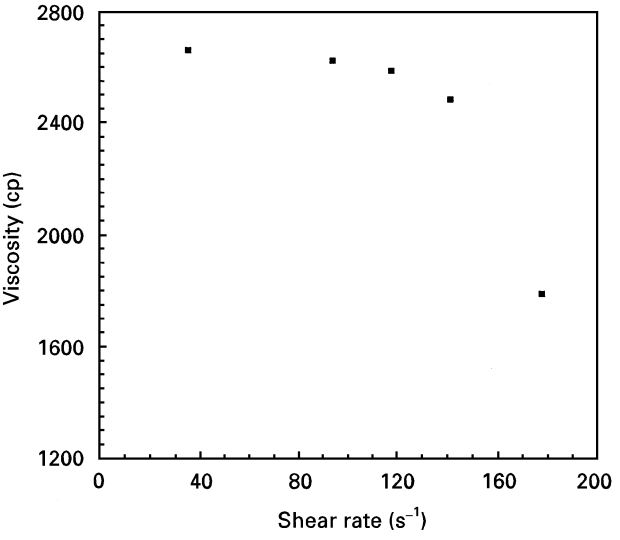

Figure 2 Effect of shear rate on the viscosity of A356 alloy. The melt was stirred at 873 K for 60 s at various shear rates, with 15 s rest time after stirring.

effect, resulting in the Oswald ripening [15] phenomenon, which would be enhanced by stirring due to accelerated solute diffusion. Two competing mechanisms also prevail, which are structure agglomeration due to bond formation among particles caused by impingement and reaction, and subsequent structure breakdown due to shearing and particle collision [2]. As a result, the balance between dendrite fragmentation, Oswald ripening, and structure agglomeration and breakdown governs the structure revolution. The dendrite fragmentation mechanism becomes less and less prevalent, as particles become further spheroidized. When the agglomeration mechanism dominates over the breakdown mechanism, a second "rosette" type of structure, due to particle coalescence, may develop. A steady state may be eventually reached where the structure agglomeration and breakdown mechanisms are balanced, after which

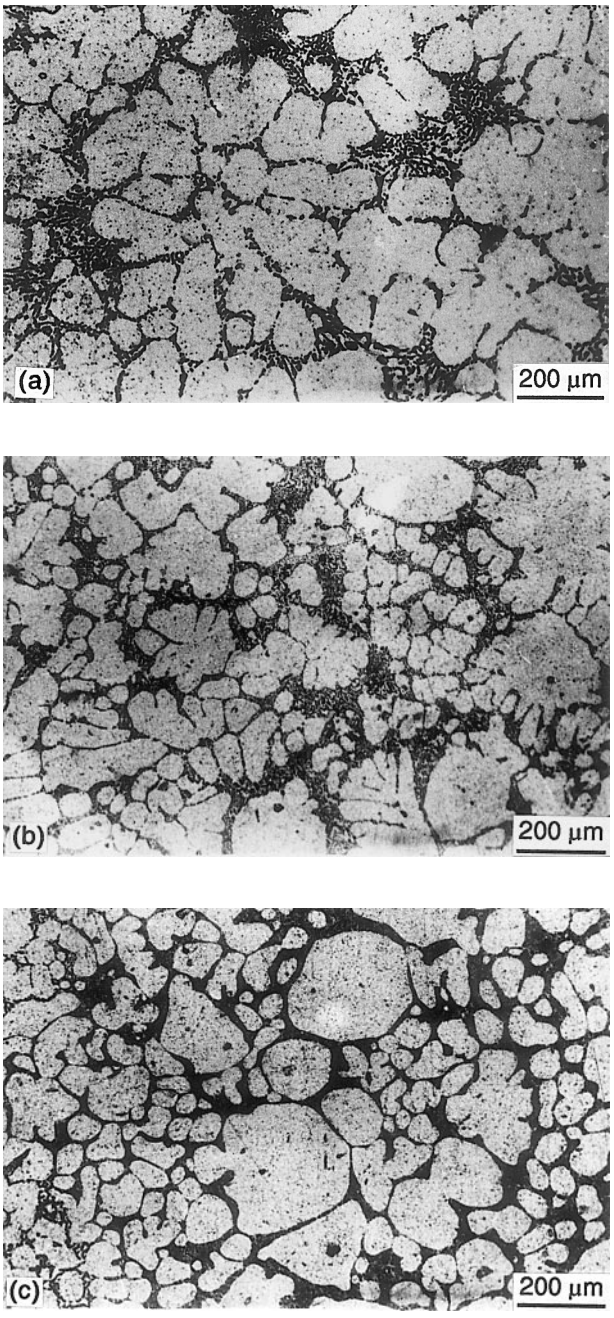

Figure 3 Variations of the structure stirred at 873 K for 60 s at (a) 95 s^{-1}, (b) 119 s^{-1}, and (c) 142 s^{-1} shear rates, with 15 s rest time after stirring.

Oswald ripening might become the prevalent mechanism [15].

The average grain sizes are 82, 54 and 46 μm for 95, 119 and 142 s^{-1} shear rates, respectively, indicating that the average grain size decreases as the shear rate increases for short stirring time, 60 s, because in the initial stage of stirring, the dendrite fragmentation dominates, for which a higher shear rate would lead to a smaller particle size. The smaller the particles, the lower the viscosity due to the greater ease with which smaller particles slide by each other without directly impacting, than for larger particles. The sphericities are 0.604, 0.612, and 0.68 for 95, 119 and 142 s^{-1} shear rates, respectively, indicating that the sphericity increases as the shear rate increases, because the two aforementioned spheroidizing mechanisms, i.e. particle shearing/abrasion and the reduction of the interfacial area, were enhanced by the higher shear rate.

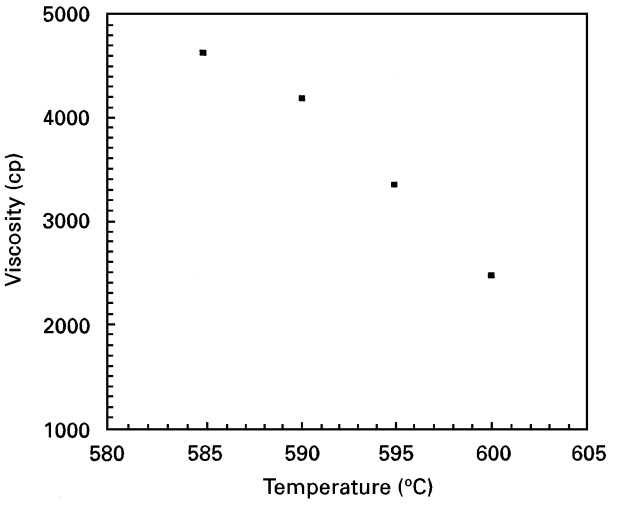

Figure 4 Effect of temperature on the viscosity of A356 alloy. The melt was stirred at various temperatures for 60 s at 119 s^{-1} shear rate, with 15 s rest time after stirring.

Fig. 4 shows the effect of temperature on the viscosity of A356 alloy, which was superheated 50 K over the liquidus, at which temperature the melt was held for 5 min before being cooled to 873, 868, 863 and 858 K, respectively, at a rate of 0.5 K min^{-1}, and the melt was isothermally stirred at 119 s^{-1} shear rate for 60 s, then held unstirred for 15 s before viscosity was measured and the samples were taken. The viscosity increases as temperature decreases due to higher solid fraction and larger crystal size, as shown in Fig. 5, which is believed to be due to the growth and coarsening of the crystals as temperature decreases. The spheroidizing effect is not significant for such a short stirring time.

Fig. 6 shows the effect of rest time on the viscosity of A356 alloy, which was superheated 50 K over the liquidus, at which temperature the melt was held for 5 min before being cooled to 873 K at a rate of 0.5 K min^{-1}, and the melt was isothermally stirred at 119 s^{-1} shear rate for 60 s, then held unstirred for various times before the viscosity was measured and the samples were taken. The viscosity increases as the rest time increases, because the crystals coarsen as the rest time, following stirring, increases as shown in Fig. 7, and the larger the crystals, the higher is the viscosity due to the greater difficulty and less chance for sliding among the crystals. The average grain sizes are 15, 24, 31, 444 and 444 μm for 60, 300, 660, 1800 and 2100 s rest time, respectively, the coarsening exponent for which, according to LSW theory [16, 17], was calculated to be 3.2, indicating that the coarsening of particles during the rest time following stirring is controlled by the particle volume diffusion [16–19]. The average sphericities are 0.661, 0.721, and 0.785 for 60, 300, 660, 1800 and 2100 s rest time, respectively, indicating that the sphericity increases as the rest time increases because the spheroidizing mechanisms were able to be in operation for a longer time.

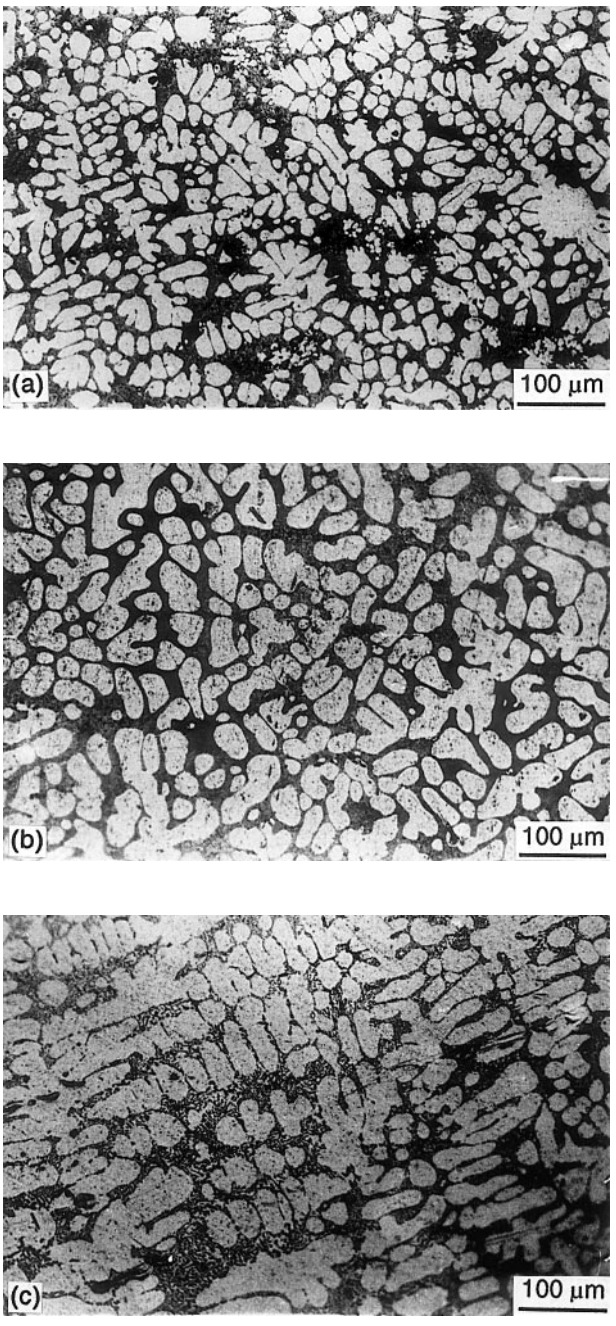

Figure 5 Variations of the structure stirred at (a) 873 K, (b) 868 K, and (c) 863 K, for 60 s at 119 s^{-1} shear rate, with 15 s rest time after stirring.

Fig. 8 shows the effect of stirring time on the viscosity of A356 alloy, which was superheated 50 K over the liquidus, at which temperature the melt was held for 5 min before being cooled at 873 K at a rate of 0.5 K min^{-1}, and the melt was isothermally sheared at 119 s^{-1} shear rate for various increments of time, then held unstirred for 15 s before the viscosity was measured and the samples were taken. Fig. 9 shows the corresponding micrographs for stirring times of 30, 150, 300 and 600 s, respectively. The structure at 30 s is still mainly dendritic. The average grain sizes are 16, 16 and 10 μm for 150, 300 and 600 s stirring times, respectively. In the presence of stirring, where liquid convection and grain rotation must be considered, Wan and Sahm [15, 20] have shown that the grain size increases as stirring time increases. However, in the present study, the grain size decreases as stirring time increases. We believe that in the present study, the stirring time of less than 600 s is still in the initial stage of stirring where the dendrite fragmentation mechanism is dominant, resulting in a smaller grain size as stirring time is increased. It is also proposed that there is a critical stirring time,

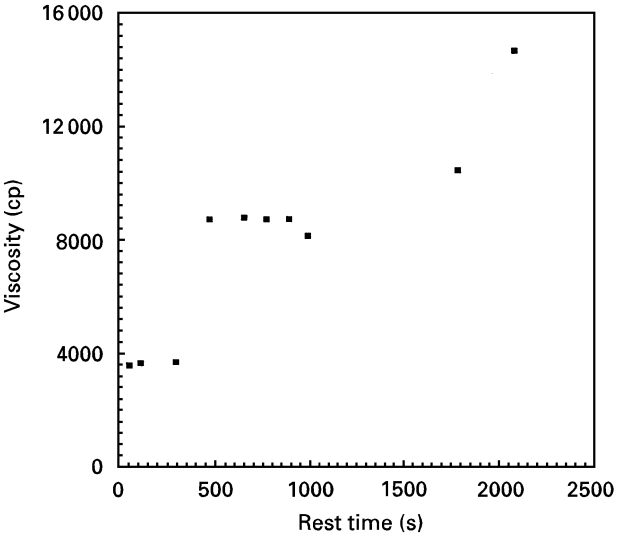

Figure 6 Effect of rest time on the viscosity of A356 alloy. The melt was stirred at 873 K for 60 s at 119 s^{-1} shear rate, with various rest times after stirring.

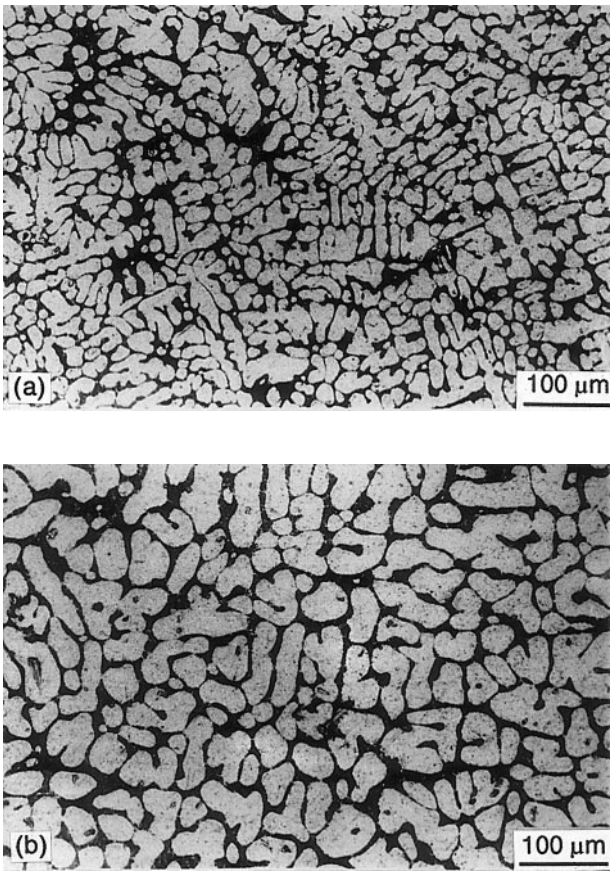

Figure 7 Variations of the structure stirred at 873 K for 60 s at 119 s^{-1} shear rate with (a) 60 s, (b) 300 s, (c) 660 s, (d) 1800 s, and (e) 2100 s rest time after stirring.

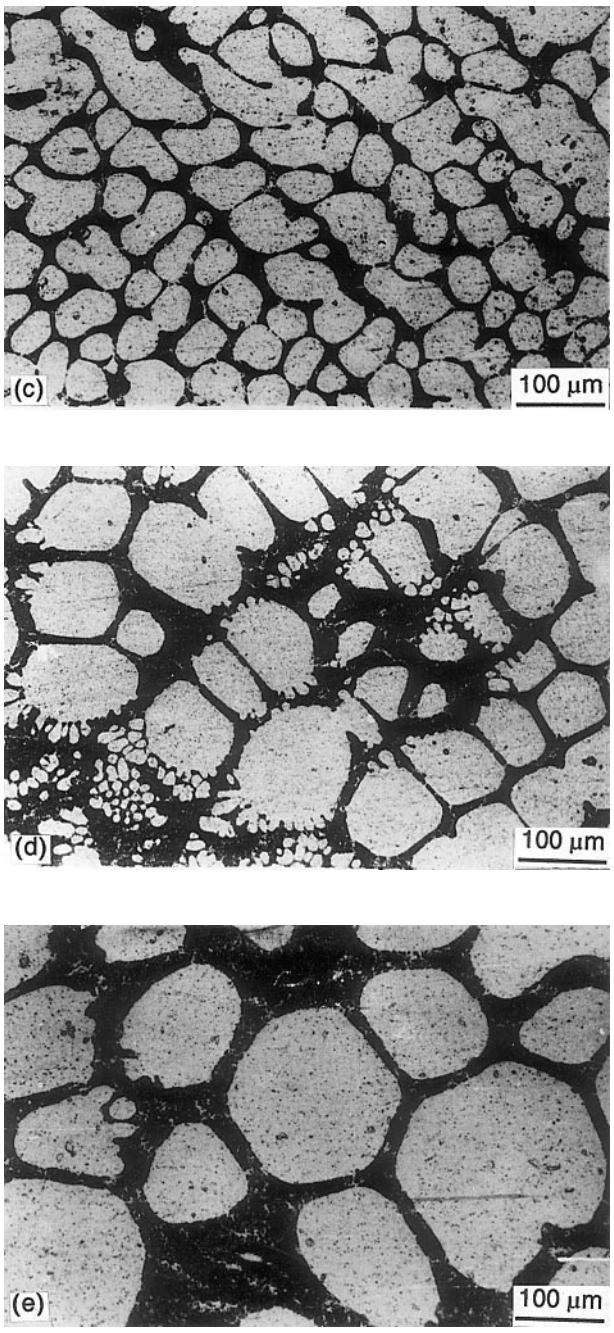

Figure 7 (Continued)

above which the grain size increases with stirring time, and below which the grain size decreases with stirring time. As a result, the viscosities are the same for 150 and 300 s stirring times, because the grain sizes are the same for both stirring times. However, the viscosity decreases significantly at 600 s due to a smaller grain size. The sphericity increases as the stirring time increases because the spheroidizing mechanisms were able to be in operation for a longer time.

4. Conclusions

1. During continuous cooling, the viscosity increases slowly at the onset of the semi-solid region, and starts to increase abruptly after reaching a critical temperature. The higher the shear rate, the lower is the critical temperature.

2. During isothermal stirring, the viscosity decreases and the sphericity increases as the shear rate increases. The grain size decreases and the sphericity increases as the shear rate increases for short stirring times.

3. The viscosity increases as the temperature decreases during isothermal stirring. The spheroidizing effect is not significant for short stirring times.

4. During isothermal stirring, the viscosity increases as the rest time increases. Both the grain size and sphericity increase as the rest time, following

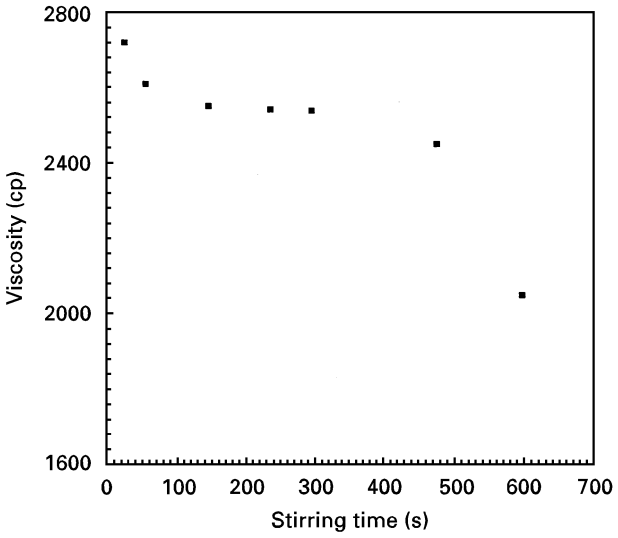

Figure 8 Effect of stirring time on the viscosity of A356 alloy. The melt was stirred at 873 K for various times at 119 s^{-1} shear rate, with 15 s time after stirring.

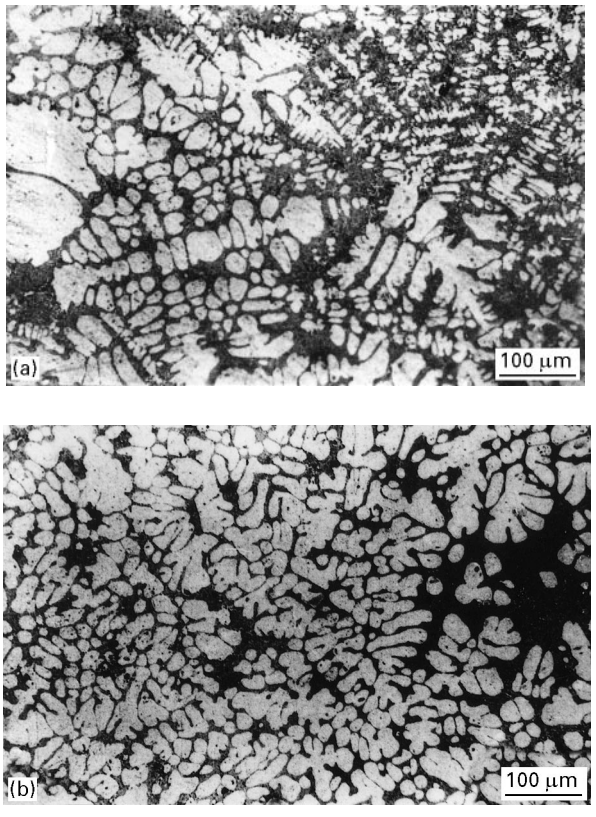

Figure 9 Variations of the structure stirred at 873 K for (a) 30 s, (b) 150 s, (c) 300 s, and (d) 600 s at 119 s^{-1} shear rate with 15 s rest time after stirring.

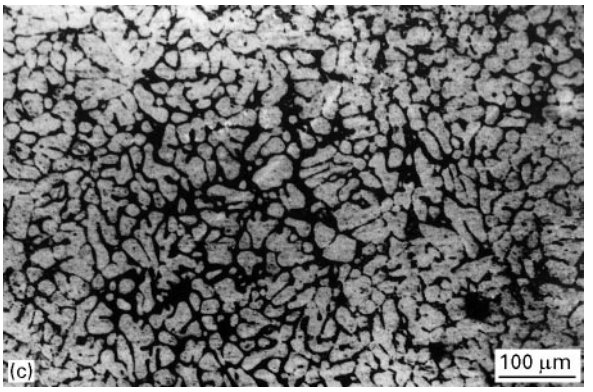

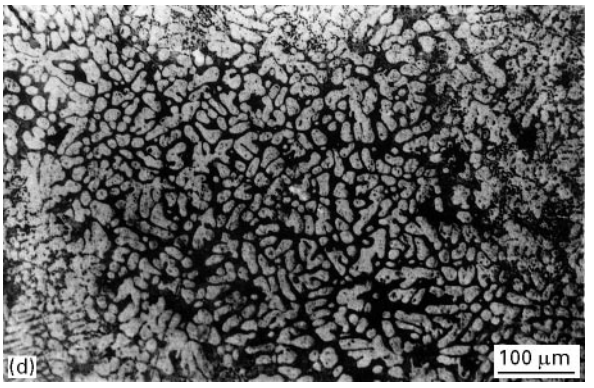

Figure 9 (Continued)

stirring, increases. The coarsening exponent is 3.2, suggesting that the coarsening is controlled by the volume diffusion of the grains.

5. During isothermal stirring, the viscosity decreases as the stirring time increases. The sphericity increases and the grain size decreases as the stirring time increases. We propose that there is a critical stirring time, above which the grain size increases with stirring time, but below which the grain size decreases with stirring time.

Acknowledgement

Support from the National Science Council of Taiwan under grant NSC 84-2216-E006-034 is gratefully acknowledged.

References

1. M. P. KENNY, J. A. COURTOIS, R. D. EVANTS and G. M. FARRIOR, "Metals Handbook", edited by D. M. Stefanescu, J. R. Davis, J. D. Destefani, T. B. Zorc, H. J. Frissell, G. M. Crankovic and A. W. Ronke. (ASM International, OH, USA, 1988) Vol. 15, 9th edn, pp. 327–38.
2. M. C. FLEMING, *Metal. Trans.* **22A** (1991) 957.
3. M. C. FLEMINGS, R. G. RIEK and K. P. YOUNG, *Mater. Sci. Eng.* **25** (1976) 103.
4. S. B. BROWN and M. C. FLEMINGS, *Adv. Mater. Process.* **6** (1993) 36.
5. W. W. SUNDGUIST, *ibid.* **6** (1993) 29.
6. D. B. SPENCER, R. MEHRABIAN and M. C. FLEMINGS, *Metall. Trans.* **3** (1972) 1925.
7. N. HAN, G. POLLARD and R. STEVENS, *Mater. Sci. Technol.* **8** (1992) 52.
8. M. SUERY and M. C. FLEMINGS, *Metall. Trans.* **13A** (1982) 1809.
9. J. F. SECONDE and M. SUERY, *J. Mater. Sci.* **19** (1984) 3995.
10. V. LAXMANAN and M. C. FLEMINGS, *Metall. Trans.* **11A** (1980) 1927.
11. D. A. PINSKY, P. O. CHARREYRON and M. C. FLEMINGS, *ibid.* **15B** (1984) 173.
12. P. O. CHARREYRON and M. C. FLEMINGS, *Int. J. Mech. Sci.* **7** (1985) 781.
13. C. P. CHEN and C.-Y. A. TSAO, *J. Mater. Sci.* **30** (1995) 4019.
14. R. B. BIRD, W. E. STEWARD and E. N. LIGHTFOOT, "Transport Phenomena" (Eurasia) p. 42
15. G. WAN and P. R. SAHM, *Acta Metall. Mater.* **38** (1990) 967.
16. I. M. LIFSHITZ and V. V. SLYOZOV, *J. Phys. Chem. Solids* **11** (1961) 35.
17. C. WAGNER, *Z. Electrochem.* **65** (1968) 581.
18. M. V. SPEIGH, *Acta Metall.* **16** (1968) 133.
19. A. J. ARDELL, *ibid.* **20** (1972) 601.
20. G. WAN and P. R. SAHM, *Acta Metall. Mater.* **38** (1990) 2367.

Received 19 January
and accepted 8 May 1996